Demonstration of polarization pulling using a fiber-optic parametric amplifier

B. Stiller,[1] **P. Morin,**[2] **D. M. Nguyen,**[1] **J. Fatome,**[2] **S. Pitois,**[2] **E. Lantz,**[1] **H. Maillotte,**[1] **C. R. Menyuk,**[3] **and T. Sylvestre**[1,*]

[1]*Institut FEMTO-ST, Département d'Optique, UMR 6174 CNRS-Université de Franche-Comté, 25000 Besançon, France*
[2]*Laboratoire Interdisciplinaire Carnot de Bourgogne, UMR 6303 CNRS, Université de Bourgogne, 21078 Dijon, France*
[3]*Department of Computer Science and Electrical Engineering, University of Maryland, Baltimore, MD 21250, USA*

[*] *thibaut.sylvestre@univ-fcomte.fr*

Abstract: We report the observation of all-optical polarization pulling of an initially polarization-scrambled signal using parametric amplification in a highly nonlinear optical fiber. Broadband polarization pulling has been achieved both for the signal and idler waves with up to 25 dB gain using the strong polarization sensitivity of parametric amplifiers. We further derive the probability distribution function for the final polarization state, assuming a randomly polarized initial state, and we show that it agrees well with the experiments.

© 2012 Optical Society of America

OCIS codes: (190.4370) Nonlinear optics, fibers; (190.4970) Parametric oscillators and amplifiers; (230.5440) Polarization-selective devices.

References and links

1. S. Pitois, J. Fatome, and G. Millot, "Polarization attraction using counter-propagating waves in optical fiber at telecommunication wavelengths," Opt. Express **16**(9), 6646–6651 (2008).
2. J. Fatome, P. Morin, S. Pitois, and G. Millot, "Light-by-Light Polarization Control of 10-Gb/s RZ and NRZ Telecommunication Signals," IEEE J. Sel. Top. Quant. Electron. **18**(2), 621–628 (2012).
3. V. V. Kozlov, J. Nuno, and S. Wabnitz, "Theory of lossless polarization attraction in telecommunication fibers," J. Opt. Soc. Am. B **28**(1), 100–108 (2011).
4. M. Martinelli, M. Cirigliano, M. Ferrario, L. Marazzi, and P. Martelli, "Evidence of Raman-induced polarization pulling," Opt. Express **17**(2), 947–955 (2009).
5. L. Ursini, M. Santagiustina, and L. Palmieri, "Raman Nonlinear Polarization Pulling in the Pump Depleted Regime in Randomly Birefringent Fibers," IEEE Photon. Technol. Lett. **23**(4), 1041–1135 (2011).
6. Z. Shmilovitch, N. Primerov, A. Zadok, A. Sanghoon Chin, L. Thevenaz, and M. Tur, "Dual-pump push-pull polarization control using stimulated Brillouin scattering," Opt. Express **19**, 25873–25880 (2011).
7. M. E. Marhic, *Fiber Optical Parametric Amplifiers, Oscillators and Related Devices* (Cambridge University Press, Cambridge 2007).
8. J. F. L. Freitas, C. J. S. de Matos, M. B. Costa e Silva, and A. S. L. Gomes, "Impact of phase modulation and parametric gain on signal polarization in an anomalously dispersive optical fiber," J. Opt. Soc. Am. B **24**(7), 1469–1474 (2007).
9. M. Guasoni and S. Wabnitz, "Nonlinear polarizers based on four-wave mixing in high-birefringence optical fibers," J. Opt. Soc. Am. B **29**, 1511–1520 (2012).
10. Q. Lin and G. P. Agrawal, "Vector theory of four-wave mixing: polarization effects in fiber-optic parameteric amplifiers," J. Opt. Soc. Am. B **21**, 1216–1224 (2004).
11. A. Durécu-Legrand, C. Simmoneau, D. Bayart, A. Mussot, T. Sylvestre, E. Lantz, and H. Maillotte, "Impact of pump OSNR on noise figure for fiber-optical parametric amplifiers," IEEE Photon. Technol. Lett. **17**(6), 1178–1180 (2005).

12. N. A. Silva, N. J. Muga, and A. N. Pinto, "Influence of the Stimulated Raman Scattering on the Four-Wave Mixing Process in Birefringent Fibers," J. Lightwave Technol. **27**(22), 4979–4988 (2009).
13. A. Zadok, E. Zilka, A. Eyal, L. Thevenaz, and M. Tur, "Vector analysis of stimulated Brillouin scattering amplification in standard single-mode fibers," Opt. Express **16**(26), 21692–21707 (2008).
14. C. R. Menyuk, D. Wang, and A. N. Pilipetskii, "Repolarization of polarization-scrambled optical signals due to polarization dependent loss," IEEE Photon. Technol. Lett. **9**(9), 1247–1249 (1997).

1. Introduction

In the last few years, several authors have reported all-optical polarization attraction of light using nonlinear optical effects in fibers [1–6]. Nonlinear polarization pulling appears to be a promising solution for photonic applications requiring high-precision polarization control and thus opens up a new means to fully control the state of polarization (SOP) without adding polarization-dependent losses (PDL), as in conventional polarization controller devices. So far, nonlinear polarization pulling has been demonstrated using counterpropagating pump waves [1–3], stimulated Raman scattering [4, 5] and stimulated Brillouin scattering [6].

As the parametric amplification is a highly polarization dependent phenomenon, one can also expect to observe a polarization pulling process in such a device [7–10]. However, except in refs. [8] and [9], where FOPA-based polarization pulling was previously predicted and theoretically analyzed, fiber-based parametric amplifiers (FOPAs) have mostly been used to date in polarization insensitive applications for optical communications and not for their strong polarization sensitivity [7]. In this work, we report the experimental demonstration of polarization pulling of an initially polarization-scrambled signal using a FOPA [7]. Nonlinear polarization pulling has been achieved for both the signal and idler waves over a broad bandwidth using the strong polarization-dependent gain (PDG) of parametric amplifiers [7]. We further provide a theoretical approach based on PDG that agrees well with our experimental results.

2. Experimental setup

The experimental setup of the fiber-optic parametric polarizer is depicted in Fig. 1. Two linearly-polarized continuous-wave (CW) external cavity tunable lasers are used as the signal and pump sources. The pump laser was spectrally broadened with a $LiNbO_3$-based phase modulator driven by a $2^{23}-1$ pseudorandom bit sequence at a fundamental frequency of 3 GHz in order to suppress stimulated Brillouin scattering while keeping a constant CW power. Using a high-resolution optical spectrum analyzer, we measured the broadened pump linewidth to be $\Delta v_p \approx 3$ GHz. The output was launched into a high-power erbium-doped fiber amplifier (33 dBm). A 1 nm-band-pass filter then followed to reduce the amplified spontaneous emission and to keep the pump optical signal-to-noise ratio (OSNR) as high as possible [11]. The pump was coupled with the signal into the fiber parametric amplifier using a 99/1 tap fiber coupler.

For the parametric amplifier, we used a highly nonlinear fiber with a length of 490 m, a nonlinear coefficient $\gamma = 11.2 \, W^{-1} km^{-1}$, a zero-dispersion wavelength of 1553.1 nm, and a polarization mode dispersion of 0.07 $ps.km^{-1/2}$. The pump wavelength was set to $\lambda_p = 1556$ nm to provide broadband parametric gain in the small anomalous group-velocity dispersion regime of the highly nonlinear fiber and the signal wavelength was set to $\lambda_s = 1546$ nm on the peak of the anti-Stokes gain band. Since the PMD is equal to 0.07 $ps.km^{-1/2}$, over a length of 490 m, the differential group delay is 49 fs. For a signal at 1546 nm, the period of the signal is 5 fs. Hence, the frequency correlation bandwidth over which signals remain correlated in the presence of PMD is given by [(5 fs)/(49 fs)] × (1546 nm) = 158 nm. Since the pump, signal, and idler are all within 20 nm, we can ignore decorrelation due to PMD and its impact on the efficiency of the nonlinear polarization pulling. It also follows that the interaction between PMD and the Kerr nonlinearity can be neglected.

To demonstrate polarization pulling, the input signal SOP was polarization-scrambled using a commercially available polarization scrambler and the output SOP was analyzed on the Poincaré sphere by means of a polarimeter. A tunable filter is placed before the analyzer to reject most of the pump power. Output gain spectra were simultaneously recorded using another optical spectrum analyzer with 1 nm resolution. We also performed a measurement of the PDG by switching off the scrambler and by measuring the differential gain G between the maximum and minimum gains for a signal SOP parallel and orthogonal to the pump. These measurements will serve in the following for our theoretical modeling of polarization pulling.

3. Experimental results

Figure 2(a,b) shows the experimental output signal and idler SOPs (sets of 252 data points) on the Poincaré sphere for four pump powers that vary from 25.2 dBm to 29.7 dBm. The experimental values of the degrees of polarization (DOP) calculated from the Stokes parameters are indicated above each sphere. The DOP is given by [2]

$$\mathrm{DOP} = \frac{\sqrt{\langle S_1 \rangle^2 + \langle S_2 \rangle^2 + \langle S_3 \rangle^2}}{S_0}, \tag{1}$$

where S_i are the normalized Stokes parameters on the Poincaré sphere, transformed linearly so that the SOP of the pump wave is aligned with the S_3 axis. The gain spectra are also plotted in Fig. 2(c) with the parametric gain, the differential gain G and the signal OSNR in insets.

Figure 2(a,b) shows that the DOP of the signal significantly increases as the parametric gain increases, that means that the signal is simultaneously polarization-pulled and amplified, as in Raman or Brillouin amplifiers [4, 6]. We have indeed verified that the SOP of the pump wave on the Poincaré sphere is located where the polarization of the signal wave is attracted when the pump power is increased. We note that the axes of the sphere have been transformed so that the S_3-axis corresponds to the barycenter of the signal SOP measurements. The largest signal DOP is reached for the maximum parametric gain of 25 dB and a PDG of 19 dB in the undepleted pump regime while the OSNR is 22 dB. Figure 2(b) also shows that the idler SOP is pulled towards the pump with a better efficiency than the signal. This effect occurs because the idler wave is generated with a SOP that matches with the pump only due to the strict scalar phase-matching conditions [12]. Additionally, we have verified that the parametric amplified spontaneous emission is also polarized parallel to the pump with a large DOP when turning off the signal power. This behaviour is a general characteristic of nonlinear polarization pulling, in this case for the depolarized noise. This property has already been observed for FOPAs in
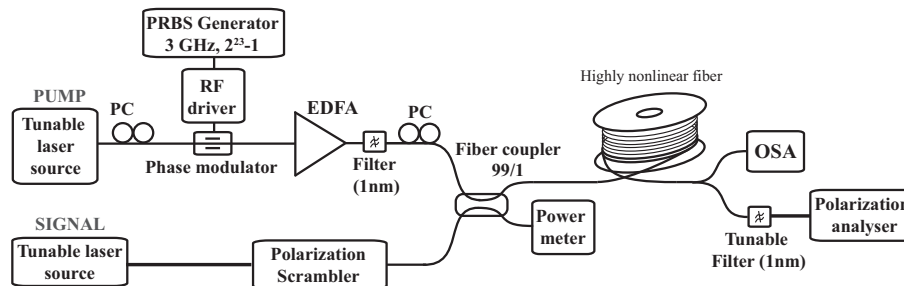

Fig. 1. Scheme of the fiber-optical parametric polarizer; PRBS Generator: pseudorandom bit sequence generator, PC: polarization controller, OSA: optical spectrum analyzer, EDFA: erbium-doped fiber amplifier.
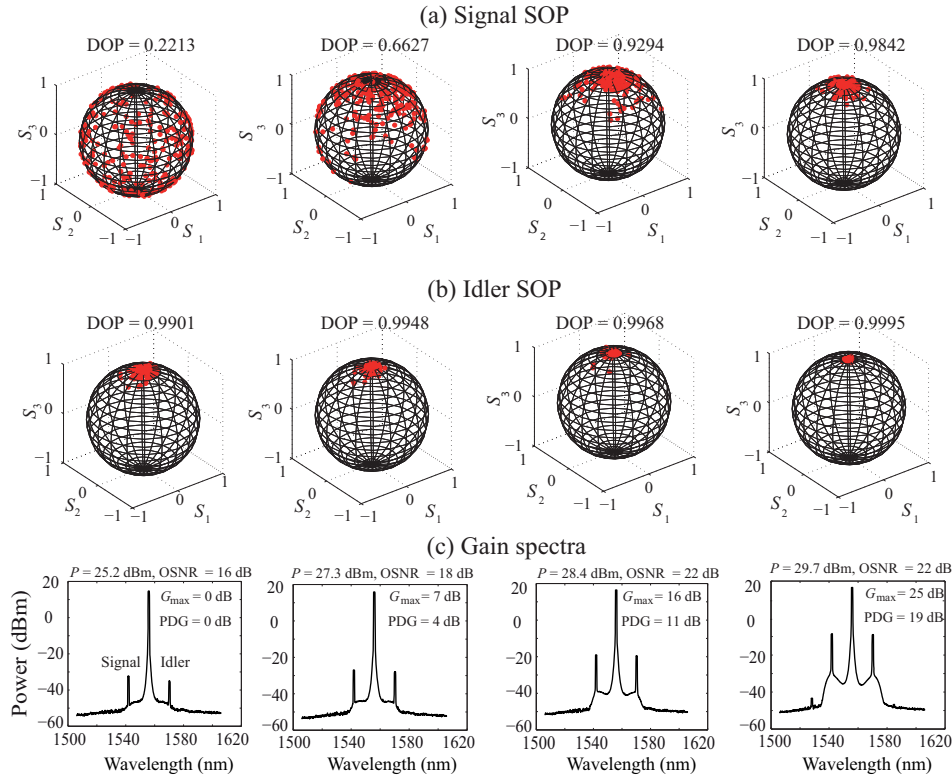
Fig. 2. Output state and degree of polarization of the (a) signal and (b) idler waves measured by a polarimeter and visualized on the Poincaré sphere while pump power increases from 25.2 dBm to 29.7 dBm from left to right. The corresponding gain spectra are shown in (c), with the input pump power P, the parametric gain G_{max}, the polarization dependent gain PDG and the signal OSNR.

noise figure measurements [11] and with respect to stimulated Brillouin scattering [13].

4. Theoretical model

We now present a theoretical model of polarization pulling based on PDG. In the Jones representation, we may write the input polarization vector as $\mathbf{u}_{in} = c_+\mathbf{u}_+ + c_-\mathbf{u}_-$, where $\mathbf{u}_+$ and $\mathbf{u}_-$ are unit Jones vectors that are aligned with the directions of maximum and minimum gain and are orthogonal [14]. Note that the SOP of the maximum and minimum gain states are not the same at the input and output of the fiber. In both cases, we effectively transform the axes of the Poincaré sphere so that the S_3-axis is aligned with the direction of maximum gain. We may usefully write $c_+ = A\cos(\theta/2)\exp(i\phi/2)$ and $c_- = A\sin(\theta/2)\exp(-i\phi/2)$, where A is the complex amplitude of the signal, while θ and ϕ are the angles of the Poincaré sphere polar coordinates. We may write

$$S_1 = \frac{2\,\mathrm{Re}(c_+c_-^*)}{|c_+|^2 + |c_-|^2} = \sin\theta\cos\phi, \qquad S_2 = \frac{2\,\mathrm{Im}(c_+c_-^*)}{|c_+|^2 + |c_-|^2} = \sin\theta\sin\phi,$$

$$S_3 = \frac{|c_+|^2 - |c_-|^2}{|c_+|^2 + |c_-|^2} = \cos\theta.$$

Thus, we find that θ is the azimuthal angle for the Stokes vector of the input signal with respect to the direction of maximum gain. It will be useful to define $\mu = \cos\theta$, so that a change in the spherical angle is given by $d\Omega = \sin\theta\,d\theta\,d\phi = d\mu\,d\phi$. It then follows that $c_+ = A\,[(1+\mu)/2])^{1/2}\exp(i\phi/2)$ and $c_- = A\,[(1-\mu)/2])^{1/2}\exp(-i\phi/2)$. We note that if the original signal is distributed uniformly over the Poincaré sphere, then the values of μ will be uniformly distributed between -1 and 1.

The output Jones vector is given by

$$\mathbf{u}_{\text{out}} = c_+\mathbf{u}_+\exp(g_+L) + c_-\mathbf{u}_-\exp(g_-L), \tag{2}$$

where g_+ and g_- are the maximum (parallel) and minimum (perpendicular) gains, respectively. The output value for μ is given by

$$\mu_{\text{out}} = \frac{|c_+|^2\exp(2g_+L) - |c_-|^2\exp(2g_-L)}{|c_+|^2\exp(2g_+L) + |c_-|^2\exp(2g_-L)} = \frac{(1+\mu) - (1-\mu)G^{-1}}{(1+\mu) + (1-\mu)G^{-1}} \tag{3}$$

where $G = \exp[2(g_+ - g_-)L]$ is the differential gain of the PDG. We note that when $G \to \infty$, we find that $\mu_{\text{out}} \to 1$, regardless of the value of μ, so that the Stokes vector is pulled to the positive S_3-axis, as we would expect.

We will calculate the probability distribution function (PDF) for μ_{out}. To do that, we first invert Eq. (3) to obtain

$$\mu = \frac{(1+G^{-1})\mu_{\text{out}} - (1-G^{-1})}{(1+G^{-1}) - (1-G^{-1})\mu_{\text{out}}}. \tag{4}$$

The quantity μ is uniformly distributed between -1 and 1, and we must have $p(\mu_{\text{out}})\,d\mu_{\text{out}} = p(\mu)\,d\mu = (1/2)\,d\mu$. We find the PDF as

$$p(\mu_{\text{out}}) = \frac{1}{2}\frac{d\mu}{d\mu_{\text{out}}} = \frac{2G^{-1}}{[(1+G^{-1}) - (1-G^{-1})\mu_{\text{out}}]^2}. \tag{5}$$

The corresponding cumulative distribution function is given by

$$F(\mu_{\text{out}}) = \int_{-1}^{\mu_{\text{out}}} p(\mu')d\mu' = \frac{1}{2} + \frac{(1+G^{-1})\mu_{\text{out}} - (1-G^{-1})}{2[(1+G^{-1}) - (1-G^{-1})\mu_{\text{out}}]} \tag{6}$$

As expected, we find that $\int_{-1}^{1} p(\mu_{\text{out}})\,d\mu_{\text{out}} = 1$, and the distribution becomes sharply peaked around $\mu_{\text{out}} = 1$ when G becomes large.

To verify the theory, we make a histogram of the S_3-component of the experimental data. We divide the interval from -1 to 1 into 21 bins with variable interval length $\Delta\mu_i = \mu_{i+1} - \mu_i$, $i = 1, 21$. The lengths of interval are chosen so that $n = 12 = 252/21$ samples lie in each interval. In Fig. 3(a), we compare the predicted PDF from Eq. (5) to the histogram height $n/(N\Delta\mu_i)$, where $N = 252$ is the total number of samples, which we plot at the mid-point of each interval, $\mu = (\mu_i + \mu_{i+1})/2$. In order to estimate the value of G, we use MATLAB's NLINFIT function to carry out a nonlinear regression analysis, based on our estimate of the cumulative distribution function $F(\mu_i, G) = N_i/N$, where $N_i = ni$ is the sum of the samples in all the histogram bins up to $\mu = \mu_i$. The expected error (standard deviation) ranges from $0.26\,\text{dB}$ to $0.44\,\text{dB}$. We note that when no parametric gain is present, we observe a negative value of G, indicating the presence of residual PDL that we attribute to the fiber couplers. As expected, an increase in the gain leads to a sharply peaked PDF in the neighborhood of $\mu_{\text{out}} = 1$ in agreement with the experiments. The agreement between the fitted values of Fig. 3(a) and the experimental maximal gain is very good, but less in comparison to the PDG. A possible reason is that the value for the PDG is biased and actually higher, since the measurement requires an accurate
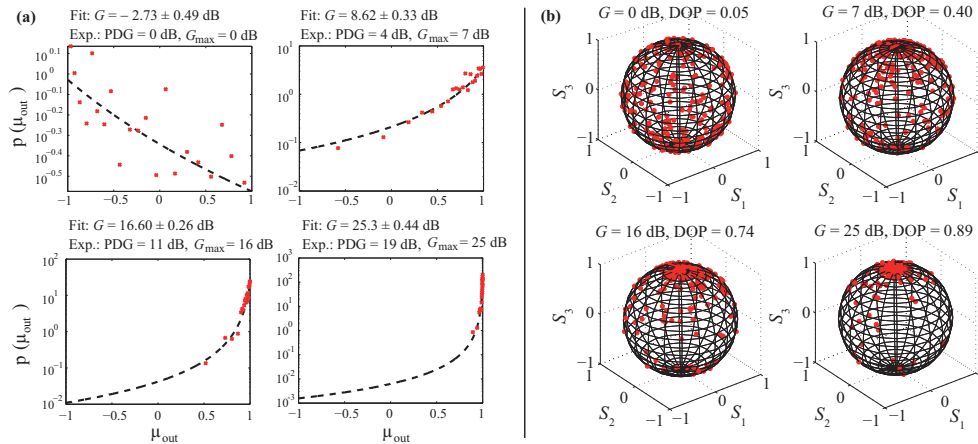
Fig. 3. (a) Probability distribution of signal S_3-component. Crosses: experimental data from Fig. 2; Dotted curves: fits by Eq. (5) with G values and standard deviation σ compared to the experimental values of PDG and the maximal gain in insets, (b) Signal output state of polarization on the Poincaré sphere calculated from Eq. (3) for the same values of G as the maximal gain in Fig 2. The DOP is indicated in the insets.

alignment of the polarization and the spectra were not sufficiently stable to accurately measure the PDG. In order to confirm this assumption we plotted in Fig. 3(b) the signal SOP on the Poincaré sphere for the same values of G as the maximal gain in Fig. 2 using Eq. (3) for S_3 and the corresponding ones for S_1 and S_2. As can be seen, the signal polarization is pulled towards the S_3-axis with increasing G. The theoretical results agree well with the experimental results in Fig. 2. However, this also confirms that the PDG in our experiment is actually higher and close to the maximal gain since the orthogonal parametric gain should be theoretically zero.

5. Conclusion

In conclusion we have proposed and demonstrated a new technique that achieves all-optical polarization control of light in optical fibers without using polarization-dependent loss, as in conventional polarizer devices. We demonstrated this technique for an initially unpolarized beam by using the strong polarization-dependent gain of a fiber-optical parametric amplifier. Both the signal and idler waves were efficiently repolarized while being parametrically ampli-fied. We have also presented a theoretical prediction for the output PDF of the DOP, assuming an unpolarized input, that agrees well with experimental results.